

# Swelling/Shrinking and Dynamic Light Scattering Studies on Chemically Cross-Linked Poly(vinyl alcohol) Gels in the Presence of Borate Ions<sup>†</sup>

Mitsuhiro Shibayama,\* Takeshi Takeuchi, and Shunji Nomura

Department of Polymer Science and Engineering, Kyoto Institute of Technology, Matsugasaki, Sakyo-ku, Kyoto 606, Japan

Received February 28, 1994; Revised Manuscript Received June 3, 1994\*

**ABSTRACT:** Swelling/shrinking behaviors of chemically cross-linked poly(vinyl alcohol) (PVA) gel complexed with borate ions were studied as a function of the borate ion concentration,  $b$ , and time. The equilibrium swelling ratio,  $Q/Q_0$ , was compared with the intrinsic viscosity ratio,  $[\eta]/[\eta]_0$ , of the corresponding PVA solutions in the presence of borate ions, where  $Q_0$  and  $[\eta]_0$  are the equilibrium swelling volume of the gel and the intrinsic viscosity of the solution without borate ions, respectively. The  $b$  dependence of  $Q/Q_0$  was almost the same as that of  $[\eta]/[\eta]_0$ . From the kinetic measurements of gel swelling and shrinking, the macroscopic diffusion coefficients for swelling and shrinking,  $D_{\text{macro}} = D_{\text{swell}}$  and  $D_{\text{shrink}}$ , respectively, were obtained. It was found that  $D_{\text{shrink}}$  is about a tenth of  $D_{\text{swell}}$ . The dynamics of a gel network were also studied by dynamic light scattering, where two types of diffusion coefficients,  $D_{\text{HT}}$  (the heterodyne method) and  $D_{\text{NE}}$  (the nonergodic medium method), were evaluated by coupling the time and ensemble-average intensity correlation functions for swollen gels. It was disclosed that  $D_{\text{swell}}$  is in good agreement with  $D_{\text{HT}}$ , not with  $D_{\text{NE}}$ . The physical meanings of  $D_{\text{HT}}$  and  $D_{\text{NE}}$  are discussed in connection with the macroscopic diffusion coefficients,  $D_{\text{swell}}$  and  $D_{\text{shrink}}$ .

## Introduction

Complexation of polymers with inorganic ions provides several interesting phenomena, such as polyelectrolyte effects on viscosity, sol-gel transition, and phase separation.<sup>1-9</sup> If a one-to-one type complexation, i.e., monocomplexation, occurs between a monomer unit of a polymer molecule and an inorganic ion, the complexed polymer chain behaves as a polyelectrolyte. However, if a dicomplexation takes place, i.e., a complexation between a monocomplex and another monomer unit of a polymer chain, a cross-link is formed. The dicomplexation leads to clustering of polymer chains, gelation, or demixing transition, depending on the spatial extent of the complexation.

Although a viscosity measurement is a useful tool so as to estimate the individual size of polymer chains in a dilute solution, an extrapolation of the reduced viscosity to the zero polymer concentration sometimes leads to a fatal error in understanding the individual polymer chain size. Particularly in the case of polyelectrolytes in aqueous solutions, a single-body problem assumption in viscosity becomes inadequate due to a long-range interaction, such as electrostatic interaction. We try to circumvent this problem using the cooperativity of gels. By introducing permanent cross-links into polymer chains, responses of polymer chains upon a change of their environment, such as temperature and ionic strength, become cooperative.

A cross-linked polymer chain network in a solvent, or in other words, a polymer gel, also allows one to visualize the change of the environment by a change of the size of the gel. Figure 1 shows a series of photographs of chemically cross-linked PVA gels prepared in a test tube. After preparation, these gels were washed with an excess amount of water for 20 days and then immersed in a solution with a prescribed amount of NaOH and B(OH)<sub>3</sub> for 130 h. The NaOH concentration, [NaOH], was 0.167

PVA-glutaraldehyde-borate Gels  
(130hr after preparation)

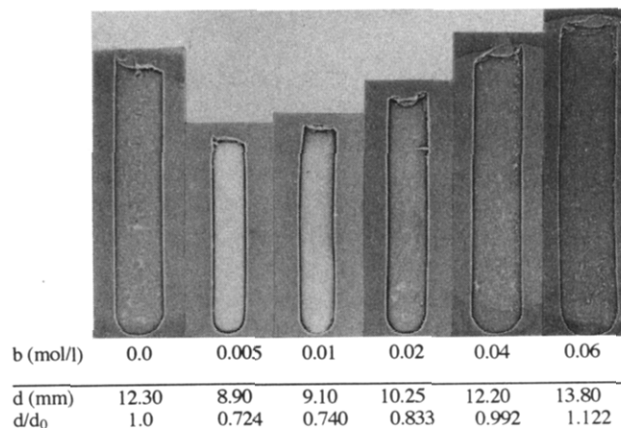


**Figure 1.** Borate concentration,  $b$ , dependence of the diameter,  $d$ , and the volume change of the gels (shown by photo).  $d_0$  is the diameter of the gel at  $b = 0$ .

N. The gel diameter,  $d$ , is listed as a function of  $b$ . The gel with  $b = 0.005$  mol/L has a smaller  $d$  than that with  $b = 0$  mol/L. However, the gel becomes larger by a further increase in  $b$ . The variation of  $d$  with  $b$  is intriguing. This is similar to the change in the intrinsic viscosity,  $[\eta]/[\eta]_0$ , observed by Ochiai et al.<sup>2</sup> for PVA-borate complexes in a dilute aqueous solution in the presence of salt. Another interesting feature is the clarity of the gel. The shrunken gels are turbid, indicating phase separation in the gel. The gel recovers its clarity in a swollen state, which is obtained with increasing  $b$ . It should be noted that the shrunken gel also became clear when it reached the equilibrium. It took for about 50 days after immersion.

Several questions are inspired from Figure 1: (a) similarity in the  $b$  dependence of the gel size,  $d$ , and of  $[\eta]/[\eta]_0$ ; (b) origin of turbidity in the shrunken regime ( $0 < b \leq 0.03$  mol/L) in the shrinking process; (c) gel swelling/shrinking kinetics; (d) microscopic views of gels in the swollen and shrunken regimes.

\* To whom correspondence should be addressed.

<sup>†</sup> Presented at the Joint Symposium on Polymer Gels and Networks, Tsukuba, Japan, Aug 31-Sept 3, 1993.

\* Abstract published in *Advance ACS Abstracts*, August 1, 1994.

The microscopic views of gels can be studied by dynamic light scattering (DLS). The cooperative diffusion coefficient,  $D_{DLS}$ , obtained by DLS is related to the correlation length of gels through the well-known mode-mode coupling theory.<sup>10-12</sup>  $D_{DLS}$  is found to be closely related to the macroscopically obtainable diffusion coefficient,  $D_{macro}$ , by a gel-swelling kinetic experiment.<sup>13-15</sup> However, it also becomes apparent that analyses of DLS on gels encounter a problem of nonergodicity since network chains in a gel are allowed only a limited Brownian motion in the phase space around their average positions.<sup>16-21</sup>

In this study, we focus on the chemically cross-linked PVA hydrogels complexed with borate ions and elucidate the cooperative nature of polymer gels in the presence of ions from both macroscopic and microscopic viewpoints. First, a comparison is made between the swelling ratio of chemically cross-linked gels and the intrinsic viscosity of the corresponding polymer solution in the presence of temporal cross-linkers, i.e., borate ions. Second, the kinetics of gel swelling/shrinking is described and the macroscopic diffusion coefficients for gel swelling/shrinking are discussed. Third, molecular dynamics of gel networks is discussed by taking account of the nature of nonergodicity. Finally, the diffusion coefficients estimated by macroscopic gel swelling/shrinking experiments are compared with those estimated by DLS.

## Theoretical Background

**1. Equilibrium Sizes of Individual Chains and Polymer Networks.** Leibler et al.<sup>4</sup> calculated the intrinsic viscosity,  $[\eta]$ , for polymer-ion complexes based on a Flory-type mean-field theory. They assumed that a polymer-ion complex comprises a random copolymer of charged and uncharged monomeric units having the monomer number fractions of  $f$  and  $1-f$ , respectively. The free energy,  $F$ , for polymer-ion complexes is given by

$$\frac{F}{kT} = \frac{3R^2}{2Na^2} + v \frac{N^2(1-f)^2}{R^3} + v' \frac{f^2 N^2}{R^3} - uK_2 \frac{f(1-f)N^2}{R^3} \quad (1)$$

where  $kT$  is the Boltzmann energy and  $R$  is the end-to-end distance of the chain having a degree of polymerization  $N$  and a monomeric length of  $a$ .  $v$  is the excluded volume, and  $v'$  is the additional excluded volume due to the electrostatic interaction,  $uK_2$ , the energy gain when a cross-link is formed. The equilibrium size of the chain is given by taking  $dF/dR = 0$ . The intrinsic viscosity is given by using the relation  $[\eta] \cong R^3/N$  and  $R_0 \cong v^{1/5} N^{3/5} a^{2/5}$  as follows:

$$\frac{[\eta]}{[\eta]_0} = \left[ (1-f)^2 + \frac{1}{2vN_A} \frac{f^2}{I} - \frac{uK_2}{v} f(1-f) \right]^{3/5} \quad (2)$$

$N_A$  and  $I$  are Avogadro's number and the ionic strength, respectively.

In the case of polymer gels at swelling equilibrium, the so-called  $C^*$  theorem<sup>12</sup> is applicable and a many-body problem for many chains can be reduced to a single-body problem for a blob having a size of  $\xi$  and a polymerization index of  $N_x$ . The free energy of the subchain in a blob is the same as that for an isolated chain of  $N = N_x$  and  $R$

$= \xi$ , and eq 2 may be rewritten as

$$\frac{F}{kT} = \frac{3\xi^2}{2N_x a^2} + v \frac{N_x^2(1-f)^2}{\xi^3} + v' \frac{N_x^2 f^2}{\xi^3} - uK_2 \frac{f(1-f)N_x^2}{\xi^3} + \ln \left( \frac{N_x^{3/2} a^3}{\xi^3} \right)^\gamma \quad (3)$$

and

$$\gamma = \xi^3(\rho_i - \rho_o) \equiv \xi^3 \Delta\rho \quad (4)$$

where  $\gamma$  is the excess number of counterions per blob in the gel.  $\rho_i$  and  $\rho_o$  are the counterion ( $=H^+$  and/or  $Na^+$ ) concentrations inside (i) and outside (o) of the gel, respectively. The fifth term on the right-hand side of eq 3 is the additional term for gel, which represents the contribution of the osmotic free energy (the translational free energy) of the counterions. In the case of a polyelectrolyte gel without salt,  $\Delta\rho$  is equal to the concentration of the charges of the polyelectrolyte, and  $\gamma$  is reduced to be the number of charges in a blob,  $fN_x$ .<sup>22,23</sup> Owing to the presence of this term, the equilibrium blob size, or the equilibrium gel size, becomes larger than that of the noncharged gel. On the contrary, when a large amount of added salt is present,  $\Delta\rho$  approaches zero and the contribution of the osmotic free energy of the counterions vanishes. In this case, eq 3 for a subchain in a blob in a gel becomes analogous to eq 1 (for a single chain in a dilute polymer solution). This is the case studied here since the concentration of the added NaOH is much larger than that of borate ions. Therefore, the ratio of the swelling equilibrium is similarly given by eq 1, and the two ratios, i.e.,  $[\eta]/[\eta]_0$  and  $Q/Q_0$ , are expected to behave similarly as a function of  $b$ .

**2. Kinetics of Swelling.** The theory of kinetics for gel swelling was first developed by Tanaka and Fillmore<sup>14</sup> for a spherical-shaped gel based on the theory for the cooperative diffusion of gels. The rate of swelling was predicted to be inversely proportional to the square of the size of the gel and was confirmed by their experiment for acrylamide gel in water. Li and Tanaka<sup>15</sup> revised the theory so as to take into account the shear modulus and proposed a theory, which predicts the effect of the shear modulus,  $\mu$ , to the net osmotic modulus in terms of the ratio,  $r$ ,

$$r \equiv \frac{\mu}{M_{os}} = \frac{\mu}{K_{os} + (4/3)\mu} \quad (5)$$

where  $\mu$ ,  $M_{os}$ , and  $K_{os}$  are the shear modulus, the longitudinal osmotic modulus, and the bulk modulus, respectively. Zrinyi et al.<sup>24</sup> employed the Li-Tanaka theory so as to describe the swelling and shrinking kinetics of chemically cross-linked poly(vinyl acetate) gels. The Li-Tanaka equation for swelling is given by

$$\frac{d(t) - d(\infty)}{d(0) - d(\infty)} = \sum_{n=1}^{\infty} B_n \exp[-t/\tau_n] \quad (6)$$

where  $d(t)$  is the diameter of the gel at time  $t$ .  $B_n$  is a complicated function of  $r$  but only dependent on  $r$  and  $\tau_n$ , the relaxation time of the  $n$ th mode. For large  $t$ , eq 6 can be expanded and truncated to

$$\ln \frac{d(t) - d(\infty)}{d(0) - d(\infty)} \cong \ln B_1 - t/\tau_1 \quad (7)$$

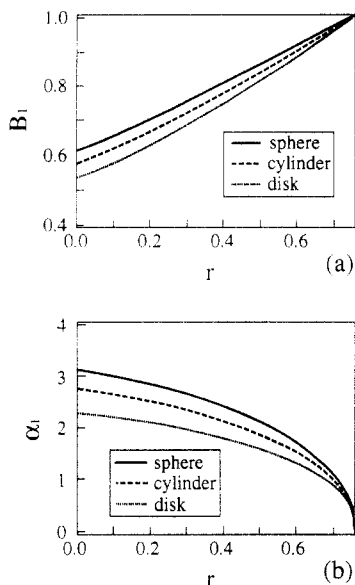


**Figure 2.** Reproduction of the theoretical curves of  $B_1$  and  $\alpha_1$  as a function of the ratio of the shear modulus to the longitudinal modulus,  $r$ , calculated by Li and Tanaka.<sup>15</sup>

The macroscopic cooperative diffusion coefficient,  $D_{\text{macro}}$ , of a gel at the surface of the gel is given by

$$D_{\text{macro}} = cd_{\infty}^2/\tau_1\alpha_1^2 \quad (8)$$

where  $\alpha_1$  is also a function of  $r$ .  $c$  is a constant dependent on the geometry of the gel, i.e.,  $c = 1, 3/2$ , and 3 for spherical-, cylindrical-, and disk-shaped gels, respectively. Figure 2 shows the reproduction of the relationship (a) between  $r$  and  $B_1$  and (b) between  $r$  and  $\alpha_1$ , which was originally given by Li and Tanaka.<sup>14</sup>

**3. Dynamic Light Scattering (DLS).** DLS data from a swollen gel were often analyzed with an assumption of ergodicity, and the cooperative diffusion coefficient and/or the correlation length were obtained based on the homodyne mode assumption.<sup>13,25–27</sup> However, the importance of the nonergodicity for viscous materials including gels was recently realized.<sup>16–21</sup> A polymer segment in a gel is allowed only a limited Brownian excursion around its average position, giving rise to a nonergodic nature. Thus the theories of DLS for nonergodic media have been extensively studied recently from both theoretical and experimental points of view. By following the treatment of Pusey et al.<sup>17</sup> and Joosten et al.,<sup>18</sup> we review and reformulate here (1) the heterodyne method and (2) the nonergodic medium method, which are employed in this study.

**(a) Heterodyne Method.** In a nonergodic medium, the scattering amplitude of each scatterer comprises the fluctuating component,  $E_f(q, \tau)$ , and the “frozen-in” constant component,  $E_c(q)$ ,

$$E(q, \tau) = E_f(q, \tau) + E_c(q) \quad (9)$$

where  $q$  and  $\tau$  are the magnitude of the scattering vector and time lag, respectively. The heterodyne method focuses only on the fluctuating component,  $E_f(q, \tau)$ , and assumes that the frozen-in component,  $E_c(q)$ , is a mere insignificant constant background. The intermediate scattering field correlation function,  $f_{\text{HT}}(q, \tau)$ , is defined for  $E_f(q, \tau)$  as follows:

$$f_{\text{HT}}(q, \tau) = \frac{\langle E_f(q, 0) E_f^*(q, \tau) \rangle_{\text{E}}}{\langle I_f(q, 0) \rangle_{\text{E}}} = \frac{\langle E_f(q, 0) E_f^*(q, \tau) \rangle_{\text{T}}}{\langle I_f(q, 0) \rangle_{\text{T}}} = 1 - D_{\text{HT}}q^2\tau + \dots \quad (10)$$

where  $I_f(q, \tau)$  is the fluctuating part of the scattered intensity, and  $\langle \rangle_{\text{T}}$  and  $\langle \rangle_{\text{E}}$  indicate the time and ensemble averages, respectively.  $D_{\text{HT}}$  is the diffusion constant evaluated with the heterodyne method. Note that the assumption of ergodicity is satisfied in this case since we treat only the fluctuating part.

The time-average normalized intensity–intensity time correlation function,  $C_{\text{T}}(q, \tau)$ , is defined by

$$C_{\text{T}}(q, \tau) \equiv \frac{\langle I(q, 0) I^*(q, \tau) \rangle_{\text{T}}}{\langle |I(q, 0)|^2 \rangle_{\text{T}}} - 1 \quad (11)$$

Note that our correlation function is different from the conventional definition,  $[f(q, \tau)]^2 + 1$ .<sup>20</sup> By defining the apparent diffusion coefficient,  $D_{\text{A}}$ ,  $C_{\text{T}}(q, \tau)$  is usually obtained in the following form:

$$C_{\text{T}}(q, \tau) = \sigma_I^2 \exp[-2D_{\text{A}}q^2\tau] + \epsilon \quad (\text{for small } \tau) \quad (12)$$

where  $\sigma_I^2$  is the initial amplitude of  $C_{\text{T}}(q, \tau)$  and  $\epsilon$  ( $\approx 0$ ) is a time-independent background in this time scale.  $C_{\text{T}}(q, \tau)$  can be rewritten with  $f_{\text{HT}}(q, \tau)$  as

$$C_{\text{T}}(q, \tau) = X^2 f_{\text{HT}}^2(q, \tau) + 2X(1 - X)f_{\text{HT}}(q, \tau) \quad (13)$$

where  $X$  is the ratio of the intensities of the fluctuating component to the total intensity as is given by

$$X \equiv \langle I_f(q) \rangle_{\text{T}} / \langle I(q) \rangle_{\text{T}} = 1 - (1 - \sigma_I^2)^{1/2} \quad (14)$$

By using the ratio  $X$ , one can relate  $D_{\text{A}}$  to  $D_{\text{HT}}$  as follows:

$$D_{\text{A}} = \frac{D_{\text{HT}}}{2 - X} = \frac{D_{\text{HT}}}{2 - \langle I_f \rangle_{\text{T}} / \langle I \rangle_{\text{T}}} \quad (15)$$

When  $X = 1$ ,  $D_{\text{A}} = D_{\text{HT}}$  and the pure homodyne mode is attained. On the other hand, for  $X = 0$ , the pure heterodyne mode is given and the relation  $D_{\text{A}} = 2D_{\text{HT}}$  is obtained. Dynamic light scattering from a gel can be regarded as a mixture of the pure homodyne and pure heterodyne modes, i.e., a partial heterodyne mode, and  $0 < X < 1$  is satisfied.

**(b) Nonergodic Medium Method.** The ensemble-average intermediate scattering field correlation function for nonergodic media,  $f_{\text{NE}}(q, \tau)$ , is defined not with the fluctuating part of the scattering amplitude but with the total scattering amplitude as

$$f_{\text{NE}}(q, \tau) = \frac{\langle E(q, 0) E^*(q, \tau) \rangle_{\text{E}}}{\langle I(q, 0) \rangle_{\text{E}}} = 1 - D_{\text{NE}}q^2\tau + \dots \quad (16)$$

In this case,  $C_{\text{T}}(q, \tau)$  is given by

$$C_{\text{T}}(q, \tau) = Y^2 f_{\text{NE}}^2(q, \tau) + 2Y(1 - Y)f_{\text{NE}}(q, \tau) \quad (17)$$

where  $Y$  is the ratio of the ensemble-average intensity to the time-average intensity,

$$Y \equiv \langle I(q) \rangle_{\text{E}} / \langle I(q) \rangle_{\text{T}} \quad (18)$$

$Y$  is equal to unity for an ergodic medium but can be a large number for nonergodic media. The connection of the three kinds of diffusion coefficients,  $D_{\text{NE}}$ ,  $D_{\text{A}}$ , and  $D_{\text{HT}}$ ,

is given as follows:

$$D_{NE} = \frac{D_A \sigma_I^2}{Y} = \frac{\sigma_I^2 \langle I(q) \rangle_T}{2 \langle I(q) \rangle_E [1 + (1 - \sigma_I^2)^{1/2}]} D_{HT} \cong \frac{\sigma_I^2 \langle I(q) \rangle_T}{2 \langle I(q) \rangle_E} D_{HT} \quad (19)$$

where  $\sigma_I^2$  was assumed to be much smaller than unity, as is the case of highly nonergodic media. Although  $D_{NE}$  is proportional to  $D_{HT}$ , the proportional constant depends on the space fluctuations,  $Y = \langle I(q) \rangle_E / \langle I(q) \rangle_T$ , as well as the initial amplitude of  $C_T(q, \tau)$ ,  $\sigma_I^2$ .

## Experimental Section

**1. Samples.** Poly(vinyl alcohol) (PVA), having a degree of polymerization of 1800, was kindly supplied by Nippon Synthetic Chemical Industry Co., Ltd. The degree of saponification was 99.96 mol %. A homogeneous PVA aqueous solution was prepared by dissolving PVA in distilled water in a water bath at 95 °C followed by rigorous stirring. Thus a homogeneous PVA solution of PVA concentration  $C_{PVA} = 50$  g/L was prepared. Then prescribed amounts of boric acid and NaOH solutions were added. The NaOH concentration was kept constant, either 0.167 or 0.333 N, throughout the experiment. These strong basic conditions guaranteed a high degree of ionization of boric acid. In the case of PVA gels, 2.5 wt % of glutaraldehyde was added to a filtered PVA aqueous solution ( $C_{PVA} = 50$  g/L), followed by a gelation in the atmosphere of an HCl acidic conditions at 30 °C for 48 h. A 10-mm-diameter test tube was used as a mold. The prepared gels were washed repeatedly with a large amount of water for 20 days. The number of cross-links is stoichiometrically estimated to be about 16 per chain. Thus a lightly cross-linked PVA gel was prepared. Then these gels were immersed in a solution of boric acid and NaOH having the same concentration as the case of the corresponding PVA solution.

**2. Viscosity Measurement and Swelling/Shrinking Measurement.** Viscosity measurements were carried out with a Ubbelohde capillary viscometer at 30 °C. The diameter of the cylindrical gel,  $d$ , was measured occasionally by taking photographs of the gels, which were prepared in a test tube and immersed in the boric acid–NaOH solution at 30 °C, as a function of time. The size of the gel was then converted to the gel volume  $Q$  by taking the cube of  $d$ .

**3. Dynamic Light Scattering (DLS).** Dynamic light scattering experiments on PVA gels were conducted with laboratory-made optics, coupled with a photon correlator, DLS-7 (a model equivalent to DLS-7000), Otsuka Electronics Co., Ltd. A 5-mW He–Ne laser was used as the incident beam. The temperature of the sample was regulated to  $20 \pm 0.1$  °C. The measurements were carried out at the scattering angle,  $\theta$ , of 60°. Data acquisition was repeated 100 times so as to gain the scattered intensity. The coherence factor,<sup>20</sup>  $\beta$ , was found to be 0.8. Ensemble-average scattered intensity  $\langle I \rangle_E$  and ensemble-average normalized intensity correlation function  $C_E(q, \tau)$  were obtained from the time-average scattered intensity  $\langle I \rangle_T$  and correlation function  $C_T(q, \tau)$  measured at 100 different sample positions (speckles) for each gel.

## Results and Discussion

**1. Static Behavior.** According to Leibler et al.,<sup>4</sup> the variation of  $[\eta]/[\eta]_0$  with the ionic strength,  $I$ , can be calculated as was done by them for PVA–borax aqueous solutions. In eq 3, the fraction of charged segments on a PVA chain,  $f$ , is given by

$$f = \frac{\bar{K}_1 C_M}{1 + \bar{K}_1 C_M} \quad (20)$$

where  $\bar{K}_1$  is the effective monocomplexation constant depending on the ionic strength and the free borate ion concentration,  $C_M$ . By using the monocomplexation

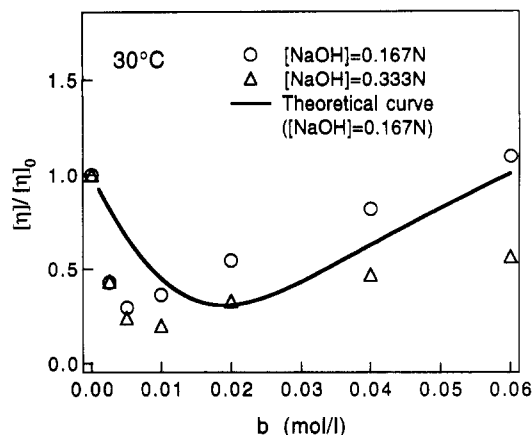


**Figure 3.**  $b$  dependence of the intrinsic viscosity ratio,  $[\eta]/[\eta]_0$ .  $[\eta]_0$  is the intrinsic viscosity of the solution without borate ions. The solid curve represents the calculated  $[\eta]/[\eta]_0$ .

constant in the absence of electrostatic effects,  $K_1$ ,  $\bar{K}_1$  is given by

$$\bar{K}_1 = K_1 \exp(-\alpha U/kT) \quad (21)$$

where  $\alpha$  is a numerical factor.  $U$  is the interaction energy between two neighboring charges induced by complexation on a chain, which is given by

$$\frac{U}{kT} = \frac{L_B}{L} \exp(-\kappa L) \quad (22)$$

$L_B$  is the Bjerrum length and  $\kappa^{-1}$  is the Debye length given by

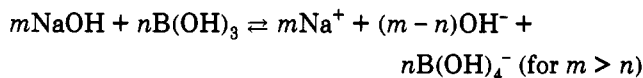
$$\kappa^2 = 8\pi N_A L_B QI \quad (23)$$

$L$  is the average spatial distance between two neighboring charges on a chain and is assumed to be a Gaussian chain as follows:

$$L = f^{1/2} a \quad (24)$$

By using the values of  $L_B = 7$  Å for aqueous solutions at 25 °C and  $a = 5$  Å, one can calculate the variation of the ratio of the intrinsic viscosities,  $[\eta]/[\eta]_0$ , as a function of ionic strength,  $I$ .

In this study, however, we should bear in mind the role of NaOH. Although NaOH behaves as a salt, the equimole of NaOH with respect to boric acid is consumed to ionize boric acid, i.e.,



where  $m$  and  $n$  are the number of moles of NaOH and  $\text{B(OH)}_3$ , respectively. Thus, whenever  $[\text{NaOH}]$  is larger than boric acid concentration,  $b$ , the ionic strength,  $I$ , is given by

$$I = \frac{1}{2} \{ [\text{Na}^+] + b + ([\text{OH}^-] - b) \} = m = [\text{Na}^+] \quad (25)$$

where we assume a full ionization of boric acid, i.e.,  $C_M = b$ .

Figure 3 shows the variations of the observed and theoretical intrinsic viscosity ratios for PVA complex solutions,  $[\eta]/[\eta]_0$ .  $[\eta]$  is normalized with respect to that for  $b = 0$ . As shown in the figure, observed  $[\eta]/[\eta]_0$  decreases with  $b$  up to  $b = 0.005$  mol/L ( $[\text{NaOH}] = 0.167$  N) or 0.01 mol/L ( $[\text{NaOH}] = 0.333$  N) and then increases

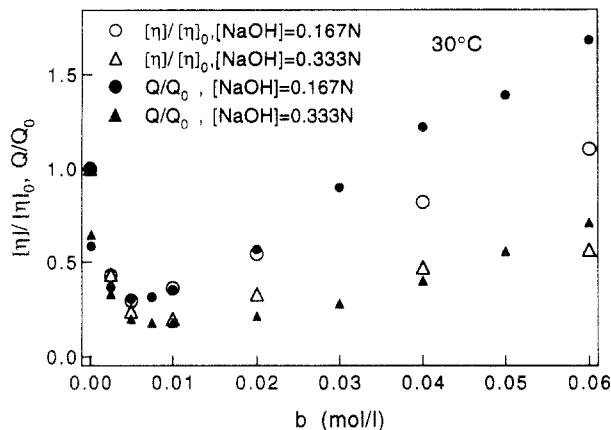
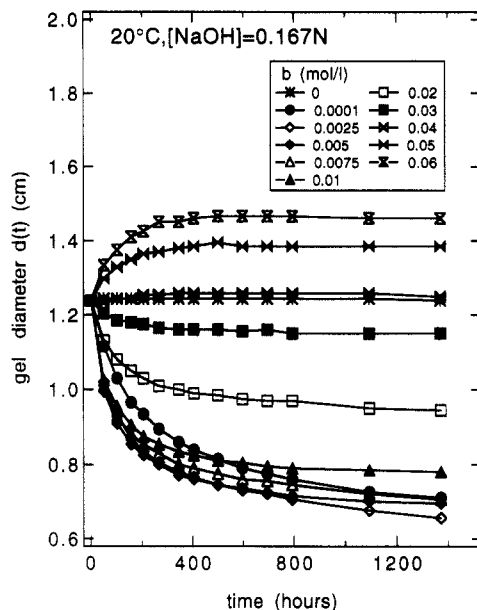


**Figure 4.**  $b$  dependence of the swelling ratio,  $Q/Q_0$ , for chemically cross-linked PVA gels as well as that of  $[\eta]/[\eta]_0$  for the corresponding PVA solutions.

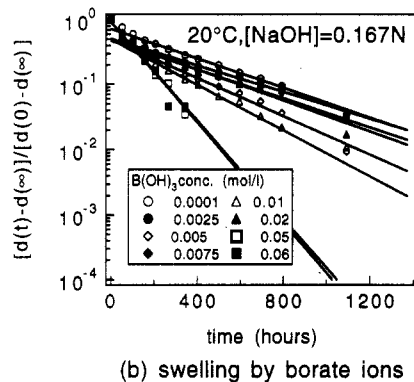
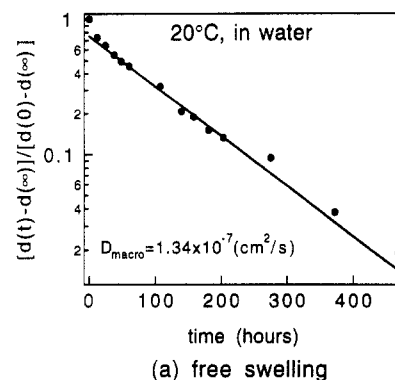
with  $b$ . The initial suppression in  $[\eta]/[\eta]_0$  is due to an intrachain cross-link formation of PVA chains.<sup>4,8</sup> The following increase in  $[\eta]/[\eta]_0$  results from a domination of the repulsive electrostatic interaction between attached borate ions on a PVA chain. The solid curve in Figure 3 represents the theoretical prediction calculated with eqs 2, 3, and 20–24, for the case of  $[\text{NaOH}] = 0.167$  N. In the calculation, we varied only  $\alpha$  since  $\alpha$  is a kind of fitting parameter in origin. Then we set  $\alpha = 2$  instead of 4 (the value used in ref 4). For other parameters, the same values as in the work by Leibler et al.<sup>4</sup> were employed; i.e.,  $K_1 = 11$  L/mol,  $v = (7 \text{ \AA})^3/2$ , and  $K_2 u N_A = 1$  L/mol, which were evaluated by other experiments. A trial for the case of  $[\text{NaOH}] = 0.333$  N was not successful because of the occurrence of a negative value in the parentheses of the right-hand side of eq 2, which indicates the collapse transition of polymer chains.<sup>8</sup> It is worth noting that the theoretical curve for  $[\text{NaOH}] = 0.167$  N roughly reproduces the experimental result for the  $b$  dependence of  $[\eta]/[\eta]_0$  with only one fitting parameter  $\alpha$ .

Figure 4 shows the comparison of the variations of  $[\eta]/[\eta]_0$  and  $Q/Q_0$  with  $b$  for the cases of  $[\text{NaOH}] = 0.167$  and  $0.333$  N. In the case of  $[\text{NaOH}] = 0.333$  N, both  $[\eta]/[\eta]_0$  and  $Q/Q_0$  behave similarly in the entire range of observation as was expected in the Theoretical Background. However, when  $[\text{NaOH}] = 0.167$  N, a systematic deviation of  $Q/Q_0$  from  $[\eta]/[\eta]_0$  is seen at high  $b$  regions, i.e.,  $0.02 \text{ mol/L} \leq b$ . This may be due to the ignorance of the fifth term of the right-hand side of eq 3. However, it can be said, at least qualitatively, that the swelling behavior of polymer gels is a macroscopic manifestation of the change of individual polymer chains in a solution as shown in Figure 4 and by the photographs in Figure 1.

**2. Swelling/Shrinking Experiment.** Figure 5 shows the time dependence of the gel diameter,  $d(t)$ , for gels immersed in solutions having different boric acid concentrations. It should be noted here that gels with  $0.0001 \leq b \leq 0.03$  mol/L shrink and those with  $b \geq 0.05$  mol/L swell with time. These behaviors are in accordance with the static behavior shown in Figure 4. The diffusion coefficient for gel swelling/shrinking was estimated with the method of Li et al.,<sup>15</sup> which takes into account the shear modulus of the gel network. For the case of  $b = 0$  mol/L, i.e., a PVA solution without borate ions,  $D_{\text{macro}}$  could not be measured by swelling experiment since no change in  $d(t)$  occurred. Therefore,  $D_{\text{macro}}$  was estimated by examining the swelling process for an unwashed gel immersed in pure water. We call this free swelling.



**Figure 5.** Time dependence of swelling/shrinking gel diameter,  $d(t)$ , for various borate concentrations,  $b$ .



**Figure 6.** Plots of the relaxation process of (a) sample FS (free swelling) and (b) sample SB (swelling by borate).

Figure 6 shows plots of the variations of  $d(t)$  for the cases of (a) free swelling (FS) and (b) swelling by borate ions (SB). The data points are well fitted with a straight line as predicted by eq 7. The ratio,  $r$  in eq 5, was evaluated from the intercept,  $B_1$  of Figure 6, followed by the estimation of  $\alpha_1$ , according to Figure 2. Then the macroscopic diffusion coefficient,  $D_{\text{macro}}$ , was obtained with eq 8, where we used  $c = 1$  (spherical gel) because of a small aspect ratio of the gel ( $\approx 2$ ). Figure 7 shows the variation of  $D_{\text{macro}}$  with  $b$ , obtained by the swelling/shrinking measurements. As shown in the figure,  $D_{\text{macro}}$  decreases dramatically by adding a small amount of boric acid and then gradually increases.  $D_{\text{macro}}$  in the shrinking mode ( $0.0001 \leq b \leq 0.03$  mol/L) is about 1 order of magnitude

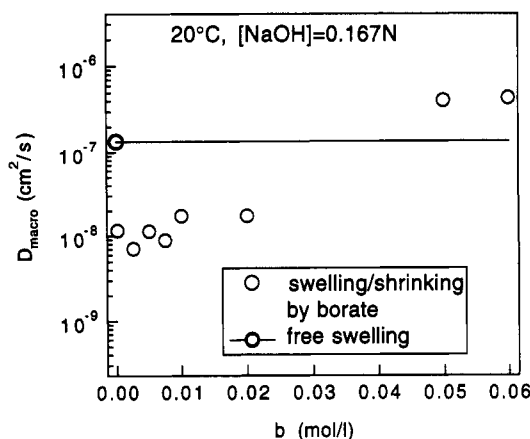


**Figure 7.**  $b$  dependence of the macroscopic diffusion coefficient,  $D_{\text{macro}}$ , obtained by swelling/shrinking experiments. The diffusion coefficient for free swelling,  $D_{\text{macro}}$ , is also shown with the horizontal line for the convenience of comparison.

**Table 1. List of the Samples for DLS Measurements**

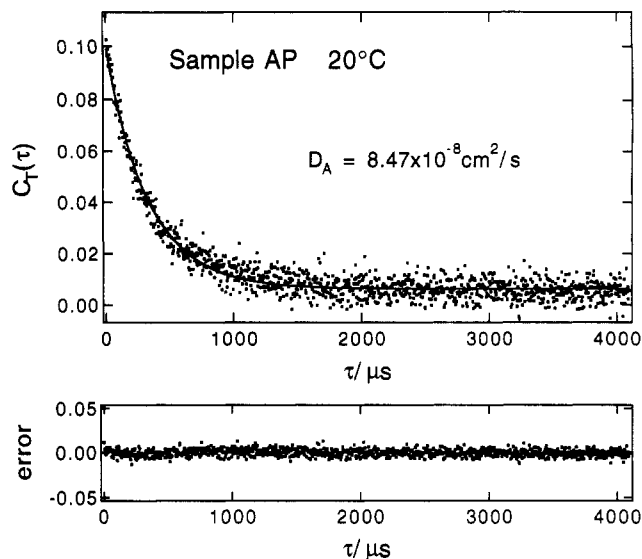
sample code	sample condition	[NaOH] (N)	$b$ (mol/L)
AP	as-prepared	0	0
FS	swelling	0	0
S0		0.167	0
S1			0.0001
S25			0.0025
S50			0.0050
S75	shrinking	0.167	0.0075
S100			0.01
S200			0.02
S300			0.03
S500	swelling	0.167	0.05
S600			0.06

smaller than that of free swelling. On the other hand,  $D_{\text{macro}}$  in the swelling mode ( $b \geq 0.05$  mol/L) is about 2 times larger than that for free swelling. This clearly indicates that the rate of swelling is much faster than that of shrinking. Formation of heterogeneity and microsyneresis may be the origin of the low rate of the cooperative diffusion for the shrunken gels.

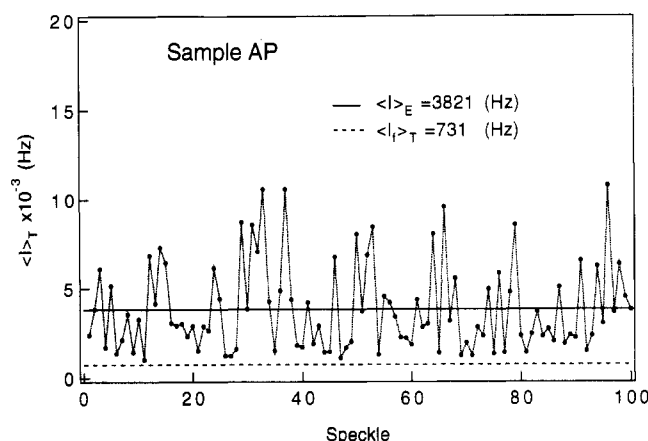
**3. Dynamic Light Scattering (DLS).** DLS measurements were conducted on the same samples studied for swelling/shrinking measurements. Table 1 lists the sample codes as well as the experimental conditions. AP and FS indicate the as-prepared sample and the free swelling sample in water, respectively. Owing to the recent advancement of the high-power Ar laser source, computer equipment, and theories, DLS data can be easily analyzed by the cumulants method, inverse Laplace transform method, and so on.<sup>20,21</sup> However, these analyses require a high reliability of the data, in other words, a high statistical reliability so as to fully analyze the correlation function in a wide time range covering several orders. Our apparatus, however, is limited in both the brilliance of the incident beam and time range of observation. Thus we employed an alternative method to evaluate the dynamics of the gel.

Figure 8 shows the intensity time correlation function,  $C_T(\tau)$ , for sample AP at 20 °C. The solid curve denotes the result of homodyne-mode curve fitting with eq 12. A nonzero value of  $C_T(\tau \rightarrow \infty)$  ( $=\epsilon$ ) indicates the presence of a long-term relaxation mode. The lower figure indicates the relative error of the fit, which is given by

$$\text{error} = \frac{C_{\text{obsd}}(\tau) - C_{\text{fitted}}(\tau)}{C_{\text{obsd}}(\tau)} \quad (26)$$



**Figure 8.** Time-average normalized correlation function of the scattered intensity,  $C_T(\tau)$ , measured at a part yielding strong time-average scattered intensity  $\langle I \rangle_T$  in sample AP.

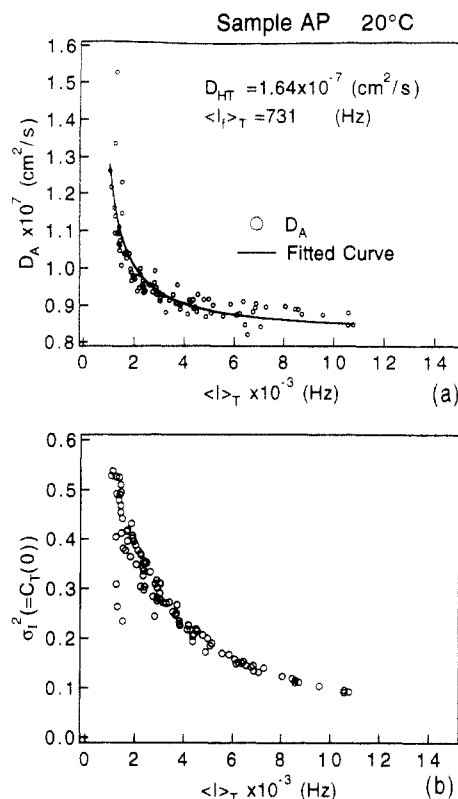


**Figure 9.** Time-average scattered intensity,  $\langle I \rangle_T$ , as a function of speckle position. The solid and dashed lines indicate the ensemble-average scattered intensity,  $\langle I \rangle_E$ , and the time-average time-fluctuating component of the scattered intensity,  $\langle I \rangle_T$ .

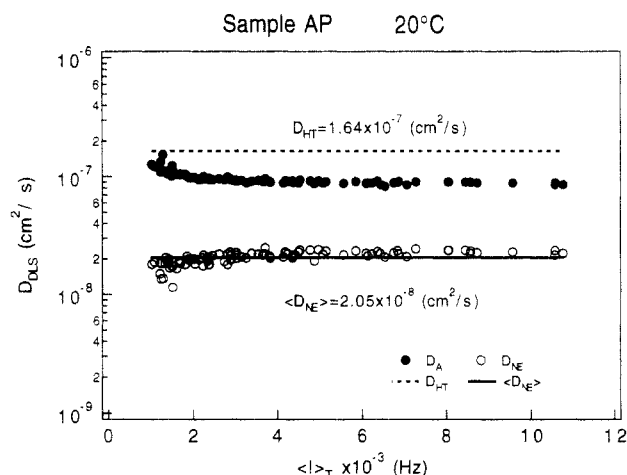
As shown in the figure, a single-exponential fit was successful although the data points are more or less scattered. The physical meaning of the apparent diffusion coefficient,  $D_A$ , is that it represents the true diffusion constant when the system is ergodic. Since  $\sigma_I^2$ , i.e.,  $C_T(\tau=0)$ , is much smaller than unity,  $X$  in eq 14 is close to 0, resulting in that the observed time correlation is not the homodyne but the heterodyne mode. This clearly indicates that the gel studied here is a highly nonergodic medium. Therefore, we measured  $C_T(\tau)$  and  $\langle I(q) \rangle_T$  at different speckles in a gel and took the ensemble average.

Figure 9 shows the time-average scattered intensity variation,  $\langle I \rangle_T$ , measured at different speckles in a gel sample AP. As shown in the figure, the scattered intensity highly fluctuates with sample position. It consists of the time-constant,  $I_c$ , and time-fluctuating components,  $I_f$ . The ensemble average,  $\langle I \rangle_E$ , is indicated with the solid line. The dashed line, the time average of the time-fluctuating component ( $I_f$ ), is obtained by plotting  $D_A$  vs  $\langle I(q) \rangle_T$ , which is shown in Figure 10a. Note the ratio of the two kinds of average intensities,  $Y$ , is 5.2, which is much larger than unity.

Figure 10 shows (a) a  $D_A$  vs  $\langle I(q) \rangle_T$  plot and (b) a  $\sigma_I^2$  vs  $\langle I(q) \rangle_T$  plot for the sample AP at 20 °C.  $D_A$  was evaluated with eq 12 and then plotted as a function of



**Figure 10.**  $\langle I \rangle_T$  dependence of (a) the apparent diffusion coefficients,  $D_A$ , and (b) the initial amplitudes,  $\sigma_l^2$ , for sample AP.



**Figure 11.** Comparison of  $\langle I \rangle_T$  dependence among  $D_{HT}$ ,  $D_{NE}$ , and  $D_A$  for sample AP.

$\langle I(q) \rangle_T$ , followed by a curve fitting with eq 15. As shown in the figure, the fitting is satisfactory.  $D_{HT}$  was thus evaluated. Figure 10b shows that the initial amplitude of  $C_T(\tau)$ ,  $\sigma_l^2$ , is widely spread between 0.1 and 0.6, suggesting that scattering from the gel is a mixture of the pure homodyne and the pure heterodyne modes. When  $\langle I(q) \rangle_T \geq 10^4$  Hz, the scattering can be regarded as the pure heterodyne mode and the relation  $D_{HT} = 2D_A$  is obtained. On the other hand, for low  $\langle I(q) \rangle_T$ , the scattering approaches the pure homodyne mode. However, we could not find such a speckle representing the pure homodyne mode.

Concurrently, we estimated the diffusion coefficient with the nonergodic medium method,  $D_{NE}$ , by taking the ensemble average of  $\langle I(q) \rangle_T$  with eq 19. Figure 11 shows the comparison among  $D_A$ ,  $D_{HT}$ , and  $D_{NE}$  for sample AP at 20 °C. Note that  $D_{HT}$  is roughly twice as large as  $D_A$ ,

indicating the scattering from the gel is near pure heterodyne. As shown in the figure,  $D_{NE}$  is about 1 order of magnitude smaller than  $D_A$  and  $D_{HT}$ , as is expected in eq 19. In addition,  $D_{NE}$  is roughly independent of  $\langle I(q) \rangle_T$ , as indicated with the solid line, the average value of  $D_{NE}$ . The macroscopically obtained diffusion constant,  $D_{macro}$ , for free swelling is  $1.4 \times 10^{-7}$  cm<sup>2</sup>/s and is roughly identical to  $D_{HT}$  within the experimental error.

It should be noted here that the rate of swelling or shrinking is much slower than that of ion complexation. The rate of ion complexation is estimated to be on the order of  $10^{-5}$  cm<sup>2</sup>/s, i.e., the same order as that of small molecules in a solution. On the other hand, that of gel swelling/shrinking estimated in this work is on the order of  $10^{-7}$  cm<sup>2</sup>/s (swelling mode) and  $10^{-8}$  cm<sup>2</sup>/s (shrinking mode). As a matter of fact, borate ions diffuse into a gel and make gel turbid within a few days. This rate is much faster (order of  $10^5$  s at the longest for a 1-cm-diameter gel) than the process of equilibration of swelling or shrinking ( $10^7$ – $10^8$  s).

**3.1. Diffusion Coefficient in the Swelling Mode.** In the swelling mode, we employed the heterodyne method. First of all, a speckle generating a high-intensity scattering was chosen. Then  $C_T(\tau)$  for the speckle was analyzed with eq 12, and  $D_A$  was converted to  $D_{HT}$  by using the relation  $X = 0$ , i.e., the pure heterodyne mode.  $D_{HT}$ 's thus estimated are listed in Table 2 as well as the diffusion coefficients,  $D_{macro}$ 's, which were macroscopically estimated by the swelling/shrinking experiment.  $D_{macro}$  for as-prepared samples (AP) and PVA gels without borate (S0) could not be conducted because the measurement required changes of gel size.  $D_{macro}$ 's for these cases are expected to be roughly equal to that of free swelling (FS). A good agreement between  $D_{macro}$  and  $D_{HT}$  was obtained for FS, S500, and S600, where gels were in the swelling mode. It was also found that the estimated  $D_{HT}$  was proportional to  $q^2$ , indicating a diffusive mode.

**3.2. Diffusion Coefficient in the Shrinking Mode.** A similar analysis was conducted for shrunken gels. The gels were kept in the borate solution for more than 2 months. The turbidity which had occurred in the beginning of the shrinking process disappeared owing to the relaxation of the strong concentration fluctuations. Thus the gels seemed to be in equilibrium. However, the DLS measurement was found to be very difficult due to the presence of a significant contribution of the frozen-in component,  $E_c(q)$ . Figure 12 shows (a) a  $D_A$  vs  $\langle I(q) \rangle_T$  plot and (b) a  $\sigma_l^2$  vs  $\langle I(q) \rangle_T$  plot for sample S25 at 20 °C, i.e., a shrunken gel. Compared to Figure 10, the range of  $\langle I(q) \rangle_T$  is much wider. This indicates that S25 gel is more heterogeneous than the sample AP. In this case,  $D_{HT}$  was not able to be estimated because the signal-to-noise ratio was remarkably low. It is needless to say that this kind of system should be studied with a combination of a high-power laser and an advanced correlator capable of detection over many orders of  $\tau$  since slow relaxation modes become significant.

**4. Interpretation of the Diffusion Coefficients Obtained by Different Methods in DLS.** In the preceding section, a discrepancy of the diffusion coefficients,  $D_{HT}$  and  $D_{NE}$ , estimated by the heterodyne and the nonergodic medium methods, respectively, became clear. In this section, we discuss the physical meanings of these diffusion coefficients in conjunction with the macroscopic diffusion coefficient,  $D_{macro}$ . According to the mode-mode coupling theory,<sup>10,11</sup> the diffusion coef-

Table 2. Comparison of  $D_{\text{macro}}$  and  $D_{\text{HT}}$ 

	AP	FS	S0	S1-S300	S500	S600
$D_{\text{macro}}$ (cm <sup>2</sup> /s)		$1.4 \times 10^{-7}$		$(0.7-1.7) \times 10^{-8}$	$4.0 \times 10^{-7}$	$4.3 \times 10^{-7}$
$D_{\text{HT}}$ (cm <sup>2</sup> /s)	$1.64 \times 10^{-7}$	$1.36 \times 10^{-7}$	$2.88 \times 10^{-7}$		$4.34 \times 10^{-7}$	$4.94 \times 10^{-7}$

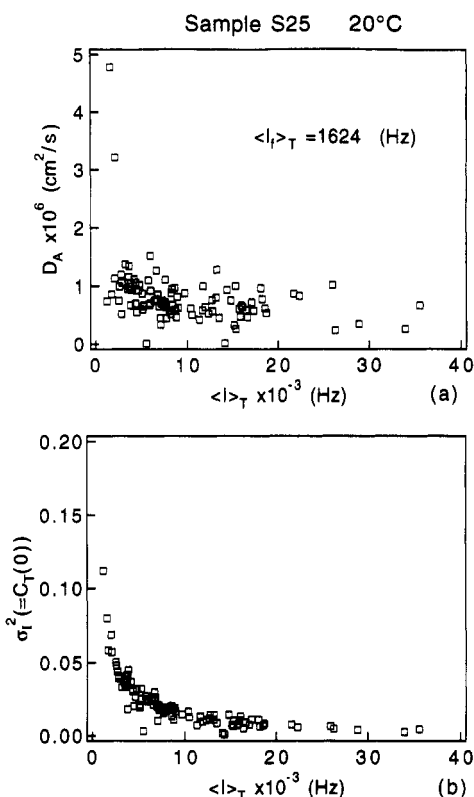


Figure 12.  $\langle I \rangle_T$  dependence of (a) the apparent diffusion coefficients,  $D_A$ , and (b) the initial amplitudes,  $\sigma_1^2$ , for sample S25 (shrunken gel).

ficient,  $D$ , is related to the correlation length,  $\xi$ , as follows:

$$D = kT/6\pi\eta_s\xi \quad (27)$$

where  $\eta_s$  is the solvent viscosity. This relation enables us to discuss the polymer concentration and cross-link concentration dependence of the diffusion coefficient. It is clear that  $f_{\text{HT}}(q, \tau)$ , defined by eq 10, accounts for the fluctuating components of the total scattering amplitude by ignoring the frozen-in component as an "uninteresting large scattering inhomogeneity".<sup>18</sup> Therefore,  $D_{\text{HT}}$  represents only the fluctuating part of a gel. This means that the concentration dependence of the correlation length in a semidilute solution may apply to a gel, at least qualitatively owing to the so-called  $C^*$  theorem,<sup>12</sup> as far as we treat a gel with the heterodyne method. Thus, the higher the gel concentration,  $C_{\text{gel}}$ , and/or cross-link concentration,  $C_x$ , the smaller the correlation length  $\xi$  we expect. Joosten et al.<sup>19</sup> studied the  $C_{\text{gel}}$  (and  $C_x$ ) dependence of these diffusion coefficients in acrylamide gels and reported that  $D_{\text{HT}}$  increases with increasing  $C_{\text{gel}}$  (and  $C_x$ ). We also obtained similar results on PVA gels as well as acrylamide gels.<sup>28</sup> These experimental results also support the interpretation of  $D_{\text{HT}}$ .

Compared to the heterodyne method, the physical meaning of  $D_{\text{NE}}$  seems to be vague. From the definition in eq 16, it is clear that the frozen-in components also contribute to the intermediate scattering field correlation function  $f_{\text{NE}}(q, \tau)$ .  $f_{\text{NE}}(q, \tau)$  represents a small excess scattering coupled with a strong frozen-in scattering. Therefore it can be deduced that  $D_{\text{NE}}$  has a contribution of the static inhomogeneity with another characteristic

scale length, such as the connectivity correlation length,  $\xi_x$ .<sup>29</sup> Although the term "connectivity correlation" was originally introduced to account for gelation threshold, we use this to represent the static inhomogeneity. Then an analogy between the correlation length and the diffusion coefficient evaluated by the two methods can be drawn as follows: The spatial correlation length,  $\xi$ , is related to  $D_{\text{HT}}$  and the connectivity correlation length,  $\xi_x$ , to  $D_{\text{NE}}$ . Then  $\xi$  and  $\xi_x$  can be rewritten as  $\xi_{\text{HT}}$  and  $\xi_{\text{NE}}$ , respectively.  $\xi_{\text{HT}}$  ( $D_{\text{HT}}$ ) and  $\xi_{\text{NE}}$  ( $D_{\text{NE}}$ ) represent the mesh size (diffusion coefficient) in the time-fluctuating part decoupled and coupled with the static inhomogeneity, respectively. Joosten et al.<sup>19</sup> observed a decrease in  $D_{\text{NE}}$  with  $C_{\text{gel}}$ , which is opposite to the behavior of  $D_{\text{HT}}$ . However, if  $D_{\text{NE}}$  is related to the connectivity correlation length, this result seems to be reasonable. The existence of large-scale static fluctuations was reported by Horkay et al. for PVA gels and poly(vinyl alcohol-*ran*-vinyl acetate) gels by the heterodyne method of DLS and static light, X-ray, and neutron scattering.<sup>30,31</sup> Fang and Brown<sup>21</sup> compared the diffusion coefficients of several kinds of gels including a PVA-water gel. They compared the diffusion coefficients obtained by the cumulants method with those obtained by the inverse Laplace transform method, by assuming several types of light scattering modes, such as homodyne, partial heterodyne, and nonergodic modes. Their conclusion was that the inverse Laplace transform method was superior by assuming the partial heterodyne mode to the cumulants method with the nonergodic mode. These experimental studies, conducted on gels in swelling equilibrium or on as-prepared gels, indicate the heterodyne method gives a proper cooperative diffusion coefficient comparable to the macroscopic diffusion coefficient.

In this study, we show that a single-exponential analysis coupled with the ensemble average well elucidates the nature of the fast mode of the gel dynamics. Although the justification of the methods presented here to analyze DLS data from nonergodic media needs further investigations, this study envisages the microscopic views of the gel networks in both swollen and as-prepared states. An investigation for microscopic views of the gel network in the shrunken mode is now in progress.

## Conclusions

Thermodynamics and kinetics of gel swelling and shrinking were studied on chemically cross-linked PVA gels in the presence of ionic cross-linker, borate ions. Dynamic light scattering experiments were also conducted on the same samples. The following facts were clarified by these macroscopic and microscopic observations:

(1) Weakly cross-linked chemical gels have a local environment similar to that of the corresponding polymer solution. This is qualitatively explained with analogy between a single chain in a dilute solution and a blob in a network when the electrostatic screening effect is dominant.

(2) The cooperative diffusion coefficient for PVA gels complexed with borate ions in the swelling mode is larger than that of free swelling (FS). On the other hand, that in the shrinking mode is a tenth as much as that of FS. In the swelling mode, borate ions accelerate the cooperative diffusion of the polymer network. However, in the shrinking mode, borate ions reduce the miscibility of PVA

in water, resulting in phase separation. A homogeneous structure is recovered after the relaxation of the concentration fluctuations. Formation of heterogeneity and microsineresis may be the origin of the low rate of the cooperative diffusion.

(3) Two kinds of diffusion coefficients,  $D_{NE}$  and  $D_{HT}$ , were obtained. The macroscopic diffusion coefficient in the swelling mode,  $D_{swell}$ , was found to be in good agreement with  $D_{HT}$ .

**Acknowledgment.** This work is supported by the Ministry of Education, Science and Culture, Japan (Grant-in-Aid Nos. 04805092, 05805080, and 06651053 to M.S.).

## References and Notes

- (1) Tsuchida, E.; Nishikawa, H. *Adv. Polym. Sci.* **1977**, *24*, 1.
- (2) Ochiai, H.; Kurita, Y.; Murakami, I. *Makromol. Chem.* **1984**, *185*, 167.
- (3) Shibayama, M.; Yoshizawa, H.; Kurokawa, H.; Fujiwara, H.; Nomura, S. *Polymer* **1988**, *29*, 336.
- (4) Leibler, L.; Pezron, E.; Pincus, P. A. *Polymer* **1988**, *29*, 1105.
- (5) Pezron, E.; Ricard, A.; Lafuma, F.; Audebert, R. *Macromolecules* **1988**, *21*, 1126.
- (6) Pezron, E.; Leibler, L.; Richard, A.; Lafuma, F.; Audebert, R. *Macromolecules* **1989**, *22*, 1169.
- (7) Pezron, E.; Leibler, L.; Lafuma, F. *Macromolecules* **1989**, *22*, 2656.
- (8) Kurokawa, H.; Shibayama, M.; Ishimaru, T.; Wu, W.; Nomura, S. *Polymer* **1992**, *33*, 2182.
- (9) Shibayama, M.; Adachi, M.; Ikkai, F.; Kurokawa, H.; Sakurai, S.; Nomura, S. *Macromolecules* **1993**, *26*, 623.
- (10) Kawasaki, K. *Ann. Phys. (N.Y.)* **1970**, *61*, 1.
- (11) Ferrell, R. *Phys. Rev. Lett.* **1970**, *24*, 1169.
- (12) de Gennes, P.-G. *Scaling Concepts in Polymer Physics*; Cornell University Press: Ithaca, NY, 1978.
- (13) Tanaka, T.; Hocker, L. O.; Benedek, G. B. *J. Chem. Phys.* **1973**, *59*, 5151.
- (14) Tanaka, T.; Fillmore, D. J. *J. Chem. Phys.* **1979**, *70*, 1214.
- (15) Li, Y.; Tanaka, T. *J. Chem. Phys.* **1990**, *92*, 1365.
- (16) Sellen, D. B. *J. Polym. Sci., Part B: Polym. Phys. Ed.* **1987**, *25*, 699.
- (17) Pusey, P. N.; van Megen, W. *Physica A* **1990**, *157*, 705.
- (18) Joosten, J. G. H.; McCarthy, J. L.; Pusey, P. N. *Macromolecules* **1991**, *24*, 6690.
- (19) Joosten, J. G. H.; Gelade, E.; Pusey, P. N. *Phys. Rev. A* **1990**, *42*, 2161.
- (20) Chu, B. *Laser Light Scattering*, 2nd ed.; Academic Press: New York, 1991.
- (21) Fang, L.; Brown, W. *Macromolecules* **1992**, *25*, 6897.
- (22) Tanaka, T.; Fillmore, D. J.; Sun, S.-T.; Nishio, I.; Swislow, G.; Shar, A. *Phys. Rev. Lett.* **1980**, *45*, 1636.
- (23) Shibayama, M.; Tanaka, T. *Adv. Polym. Sci.* **1993**, *109*, 1.
- (24) Zrinyi, M.; Rosta, J.; Horkay, F. *Macromolecules* **1993**, *26*, 3097.
- (25) Takebe, T.; Nawa, K.; Suehiro, S.; Hashimoto, T. *J. Chem. Phys.* **1989**, *91*, 4360.
- (26) Fang, L.; Brown, W.; Konak, C. *Polymer* **1990**, *31*, 1960.
- (27) Oikawa, H.; Murakami, K. *Macromolecules* **1991**, *24*, 1117.
- (28) Shibayama, M.; Fujikawa, Y.; Takeuchi, T.; Nomura, S., unpublished results.
- (29) Martin, J. E.; Wilcoxon, J. P. *Phys. Rev.* **1989**, *A39*, 252.
- (30) Horkay, F.; Burchard, W.; Geissler, E.; Hecht, A.-M. *Macromolecules* **1993**, *26*, 1296.
- (31) Horkay, F.; Burchard, W.; Hecht, A.-M.; Geissler, E. *Macromolecules* **1993**, *26*, 3375.